Cell Calcium 84 (2019) 102104

Contents lists available at ScienceDirect

Cell Calcium

journal homepage: www.elsevier.com/locate/ceca

Splice-variant-specific effects of primary aldosteronism point mutations on human $Ca_V3.2$ calcium channels

Min He, Zilan Xu, Yuchen Zhang, Changlong Hu*

Department of Physiology and Biophysics, School of Life Sciences, Institutes of Brain Science, Fudan University, Shanghai, China

ARTICLE INFO

Keywords:
$Ca_V3.2$ calcium channels
Splice-variant-specific effects
Primary aldosteronism mutations

ABSTRACT

$Ca_V3.2$ calcium channels play important roles in both neural excitability and aldosterone secretion. Recent clinical studies found four germline mutations (S196 L, M1549I, V1951E and P2083 L) in $Ca_V3.2$ channels. All four mutations caused primary aldosteronism (PA), while only the M1549I mutation resulted in obvious neural malfunctions besides PA. In human, there are two major $Ca_V3.2$ channel gene (*CACNA1H*) splice variants, either with or without exon 26. In this study, we tested the expression of the two *CACNA1H* splice variants in zona glomerulosa (ZG) cells of human adrenal cortex and the possibility that $Ca_V3.2$ (-26) and $Ca_V3.2$ (+26) channels have different functional responses to the four PA mutations. We found that human ZG cells only express long form $Ca_V3.2$(+26) channels. The M1549I mutation slowed the inactivation of $Ca_V3.2$(+26) more than 5 fold, and $Ca_V3.2$(-26) more than 2 fold. The S196 L, V1951E and P2083 L mutations accelerated channel recovery from inactivation for $Ca_V3.2$(+26), but not $Ca_V3.2$(-26) channels. All four mutations resulted in gain of function of $Ca_V3.2$(+26) channels, leading to overproduction of aldosterone. In conclusion, the four PA mutations caused more profound changes on $Ca_V3.2$ (+26) currents than on $Ca_V3.2$ (-26) currents, and except the M1549I mutation, the S196 L, V1951E and P2083 L have little effect on the electrophysiological properties of $Ca_V3.2$(-26) currents, which may partially explain the limitation of the phenotype associated with the V1951E, S196 L and P2083 L germline mutations to PA.

1. Introduction

T-type calcium channel, consisting of $Ca_V3.1$, $Ca_V3.2$ and $Ca_V3.3$ subtypes, plays important roles in various physiological and pathological processes including neuronal burst firing, cardiac pacemaking, aldosterone secretion, cardiac hypertrophy, tumor proliferation and epilepsy [1–4]. Primary aldosteronism (PA), caused by autonomous overproduction of aldosterone, is the most common single cause of secondary arterial hypertension [4]. A recent clinical study reported four germline mutations (M1549I, V1951E, S196 L and P2083 L) of $Ca_V3.2$ channel gene (*CACNA1H*) in patients with PA, while only the M1549I mutation caused obvious neural malfunctions in addition to PA, and the patient with a germline *CACNA1H* V1951E mutation was cured of PA by unilateral adrenalectomy [5]. The mechanism by which these four germline *CACNA1H* mutations lead to different clinical phenotype remains unclear.

The temporal and spatial expression patterns of voltage-gated calcium channel splice variants, and the response of individual splice variants to specific genetic mutations have been suggested to be closely related to the phenotype of channelopathies [6–8]. Jeng et al reported that the episodic ataxia type 2 mutations had obvious dominant-negative effect on the human long isoform of $Ca_V2.1$ channels(with exon 47), while physiological negligible dominant-negative effect on the short isoform of $Ca_V2.1$ channels(without exon 47) [9]. Normal adult rat heart expresses approximately equal amount of $Ca_V3.2$ with or without exon 25 splice variants, and the preferential upregulation of $Ca_V3.2$(+25) splice variant resulted in cardiac hypertrophy in hypertensive rats [10]. A previous study reported that R1584 P mutation had obvious functional effects only on rat $Ca_V3.2$ with exon 25, but not on $Ca_V3.2$ without exon 25 in rat model of absence epilepsy [11].

Two major $Ca_V3.2$ channel splice variants, either with or without exon 26 (equivalent to exon 25 in rat) (Fig. 1A) have been found in various human tissues including brain, testis, colon, prostate, kidney, uterus and ovary [9,12,13]. Aldosterone is produced by zona glomerulosa (ZG) cells of the adrenal cortex. In this study, we investigated the expression of $Ca_V3.2$ (± 26) channels in human ZG cells and studied

Abbreviations: PA, primary aldosteronism; ZG, zona glomerulosa

* Corresponding author at: Department of Physiology and Biophysics, School of Life Sciences, Institutes of Brain Science, Fudan University, 2005 Songhu Road, Shanghai 200438, China.

E-mail address: clhu@fudan.edu.cn (C. Hu).

https://doi.org/10.1016/j.ceca.2019.102104
Received 15 July 2019; Received in revised form 2 September 2019; Accepted 8 September 2019
Available online 01 November 2019

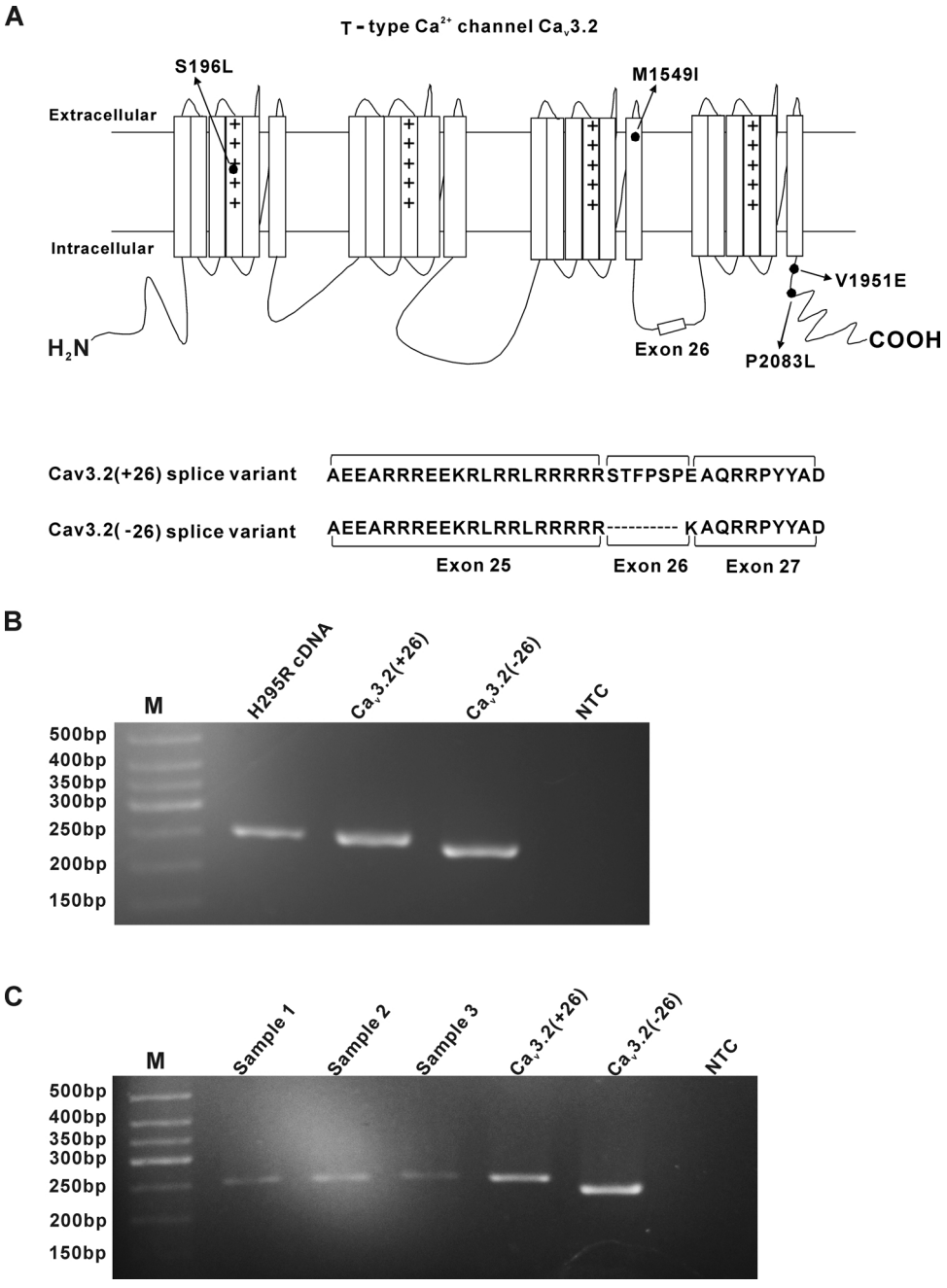

Fig. 1. The mRNA expression of $Ca_V3.2(\pm 26)$ channels in human adrenal zona glomerulosa cells. (A, B) Schematic structural models of human $Ca_V3.2$ channels with / without exon 26, and the locations of S196 L, M1549I, V1951E and P2083 L mutations. (C) RT-PCR showing the mRNA expression of $Ca_V3.2$ (+26) in human adrenocortical cell line H295R cells; $Ca_V3.2(\pm 26)$ plasmids as positive controls; NTC, no template control. (D) RT-PCR showing the expression of $Ca_V3.2$ channels in zona glomerulosa cells isolated by laser capture microdissection from three different human adrenals.

the possibility that $Ca_V3.2$ (-26) and $Ca_V3.2$ (+26) channels have different functional responses to the S196 L, M1549I, V1951E and P2083 L mutations.

2. Materials and methods

2.1. Ethics statement

Adrenal gland samples were obtained from patients undergoing radical nephrectomy to remove kidney cancer and adjacent ipsilateral adrenal as previously reported [14]. The protocol for obtaining and using human adrenal tissues in this work was approved by the Ethics Committee of School of Life Sciences (2017-601), Fudan University. Written informed consent from all patients was obtained. All protocols were in accordance with institutional guidelines.

2.2. Cell culture

Human embryonic kidney cell line, HEK293, was purchased from The Cell Bank of Chinese Academy of Science. Cells were cultured in DMEM supplemented with 10% fetal bovine serum and 1% antibiotic antimycotic solution. Antibiotic antimycotic solution, DMEM and FBS were purchased from Gibco (GIBICO, Grand Island, NY, USA). Human adrenocortical cell line, H295R (ATCC#: CRL-2128), was purchased from American Type Culture Collection. Cells were cultured in Dulbecco's Modified Eagle Medium: Nutrient Mixture F-12 medium

(GIBCO, Grand Island, NY, USA) supplemented with 10% fetal bovine serum (GIBCO), 1% antibiotic solution, and 0.1% insulin, transferrin and selenium premix (BD Biosciences, Heidelberg, Germany).

2.3. Plasmids

Plasmids for human $Ca_V3.2$ (+26) (NM_021098.2) channels in pcDNA3 plasmids were as previously reported [15]. $Ca_V3.2$ (-26) (NM_001005407.1) channels and site-directed S196 L, M1549I, V1951E and P2083 L mutageneses were achieved in the $Ca_V3.2$ channel by using the QuikChange XL Site-directed Mutagenesis kit (Stratagene, La Jolla, CA, USA). All mutations were confirmed by sequencing.

2.4. Cell transfection and electrophysiology

Plasmids for human wild-type and mutant $Ca_V3.2$ channels were transiently transfected in HEK293 cells using jetPRIME (Polyplus, Illkirch, France.) according to the manufacturer's instruction. For electrophysiological experiments, cells were used 24 h after transfection. Whole-cell currents in the HEK293 cells were recorded using an Axopatch 200B amplifier (Molecular Devices, Sunnyvale, CA, USA). The bath solution contained (in mmol/L): 143 TEACl, 10 CaCl2, 2 MgCl2, 10 HEPES, and 10 Glucose, pH 7.4 (adjusted with TEAOH). The internal solution contained (in mmol/L): 125 CsCl, 10 HEPES, 10 EGTA, 1 MgCl2, 1 CaCl2, 4 Mg-ATP, and 0.3 Tris-GTP (pH adjusted to 7.2 using CsOH). Recording pipettes had resistances of 4–6 MΩ under these solution conditions. All of the recordings were performed at room temperature. Currents were sampled at 10 kHz and filtered at 2 kHz, and corrected online for leak and residual capacitance transients using a P/4 protocol. For steady-state activation, the normalized conductances were fitted using the Boltzmann equation where $G/G_{max} = A2 + (A1-A2)/(1 + \exp((Vm-V1/2)/\text{slope factor}))$. For steady-state inactivation, the normalized currents were fitted with the following Boltzmann equation: $I/I_{max} = A2 + (A1-A2)/(1 + \exp((Vm-V1/2)/\text{slope factor}))$.

2.5. ZG cell isolation, RNA extraction and RT-PCR

The ZG layer was isolated from human adrenal glands using laser capture microdissection (Arcturus XT system, Life Technologies, Carlsbad, CA, USA). RNA was extracted using an RNeasy Micro Kit (QIAGEN Qiagen, Düsseldorf, Germany), and reversed transcribed using a SMART-Seq v4 Ultra Low Input RNA Kit (Clontech Laboratories, CA, USA). PCR was performed in 20 μL reactions containing: 2 μL of template (from 10 ng RNA), 0.4 μmol/L of each paired primer, 10 μL of 2xTaq plus PCR Master Mix(DBI Bioscience, Ludwigshafen, Germany). The thermocycling conditions were 95°C, 3 min; 35 cycles of 95°C, 15 s; 60°C, 30 s; 72°C, 30 s; and 72°C, 10 min. Primers used in PCR:$Ca_V3.2$: forward 5′ TCCTGCTCATCGTCAGCTTC 3′, reverse 5′ GGTCGAGATAG TGGCTGGTG 3′. The PCR products were run on 4% agarose gels. The PCR products for $Ca_V3.2$(-26) and $Ca_V3.2$(+26) are 231bp and 249bp respectively. Real-time polymerase chain reaction was performed in 20 μL reactions containing: 2 μL of template, 0.4 μmol /L of each paired primer, and SYBR Green Polymerase Chain Reaction master mix(Bio-Rad, Hercules, CA, USA). The thermocycling conditions were 94 °C, 2 min; 35 cycles of 95 °C, 30 s; 58 °C, 30 s; 72 °C, 1 min; and 72 °C, 5 min. Results were normalized by β-actin mRNA. Data were calculated by $2^{-\Delta\Delta Ct}$ method and reported as fold change over control. The primers used for real-time polymerase chain reaction: β-actin: forward 5′ GTGGACATCCGCAAAGAC 3′, reverse 5′ AAAGGGTGTAACGCAACTAA 3′; CYP11B2: forward 5′ CCCTCAACACTACACAGGCA 3′, reverse 5′ GTCATCAGCAAGGGAAACGC 3′; STAR: forward 5′ GCTGCTAGCGAC ATTCAAGC 3′, reverse 5′ GAGGTCGATGCTGAGTAGCC 3′.

2.6. Aldosterone secretion of H295R cells

H295R cells were transfected with wild-type and mutant $Ca_V3.2$(+26) channels for 24 h, then cells were serum deprived in Dulbecco's Modified Eagle Medium: Nutrient Mixture F-12 containing 0.1% fetal bovine serum for twelve hours. Cell culture supernatants collected after 24 h high K^+ treatment in complete medium. Medium aldosterone concentrations were analyzed using an Aldosterone ELISA Kit (ENZO Life Science, Farmingdale, NY, USA) following the manufacturer's instructions.

2.7. Statistics

Data analysis was performed with Clampfit 10.2 (Molecular Devices, Sunnyvale, CA, USA) and Origin 8.0 (OriginLab, Northampton, MA, USA). Statistical analysis consisted of unpaired Student's *t*-tests. Values are given as means ± S.E.M, n indicated the number of tested cells. $P < 0.05$ was considered statistically significant. Multiple comparisons were analyzed using a one-way ANOVA followed by *post hoc* Tukey testing.

3. Results

3.1. Effects of the four mutations on the activation properties of $Ca_V3.2$ channel currents

Two predominant *CACNA1H* splice variants, either with or without exon 26 (Fig. 1A) have been found in various human tissues including brain, testis, colon, prostate, kidney, uterus and ovary [9,12,13]. First, we investigated the mRNA expression of $Ca_V3.2(\pm 26)$ in human adrenocortical cell line H295R cells, which is the most commonly used cell model for the study of aldosterone secretion [16]. As shown in Fig. 1B, H295R cells expressed the $Ca_V3.2$(+26) but not $Ca_V3.2$(-26) splice variant. Then, we tested the mRNA expression of $Ca_V3.2(\pm 26)$ in zona glomerulosa (ZG) cells isolated from human adrenals(two men, one woman, age 36–55 years). Human ZG cells were isolated by laser capture microdissection. As shown in Fig. 1C, mRNA for $Ca_V3.2$ (+26) but not $Ca_V3.2$ (-26) was detected in human ZG cells. These data suggested that human adrenal ZG cells predominantly express the $Ca_V3.2$(+26) splice variant.

In order to investigate the effects of the four PA mutations on the electrophysiological properties of $Ca_V3.2(\pm 26)$ channels. Wild-type (WT) and mutant $Ca_V3.2(\pm 26)$ channels were transiently expressed in HEK293 cells. Fig. 2A showed typical calcium currents recorded from HEK293 cells transfected with wide-type $Ca_V3.2(\pm 26)$, S196 L and M1549I mutant $Ca_V3.2(\pm 26)$ channels. Whole cell currents were elicited by a step protocol (holding at −90 mV, depolarizing in 5-mV steps from −70 to +30 mV at 10-s intervals). All four mutations did not alter current densities of $Ca_V3.2$(+26) or $Ca_V3.2$(-26) currents (Fig. 2B and Table 1). The M1549I mutation shifted the steady-state activation curve of $Ca_V3.2$(+26) currents to hyperpolarized potentials (half-maximal voltage of activation: WT $Ca_V3.2$(+26): $V_{1/2}$ = -43.5 ± 0.7 mV; $Ca_V3.2(+26)^{M1549I}$: $V_{1/2}$ = -48.7 ± 1.3 mV, $P < 0.05$, Fig. 2C, Table 1), while did not change the activation curve of $Ca_V3.2$(-26) currents(Fig. 2C, Table 1). The other three mutations V1951E, S196 L and P2083 L did not significantly change the steady-state activation kinetics of either $Ca_V3.2$(+26) or $Ca_V3.2$(-26) currents (Fig. 2C and Table 1).

The activation time constant (Tau act) of $Ca_V3.2$(+26) currents was altered by the M1549I and P2083 L mutations (Table 1). In contrast, only the M1549I mutation produced significant change in the activation time constant of $Ca_V3.2$(-26) currents (Table 1). These data indicated that the four PA mutations produced more changes in the activation properties of $Ca_V3.2$(+26) currents than $Ca_V3.2$(-26) currents.

3.2. Effects of the four mutations on the inactivation and deactivation properties of $Ca_V3.2$ channel currents

The measurement of the time constant for inactivation (Tau inact,

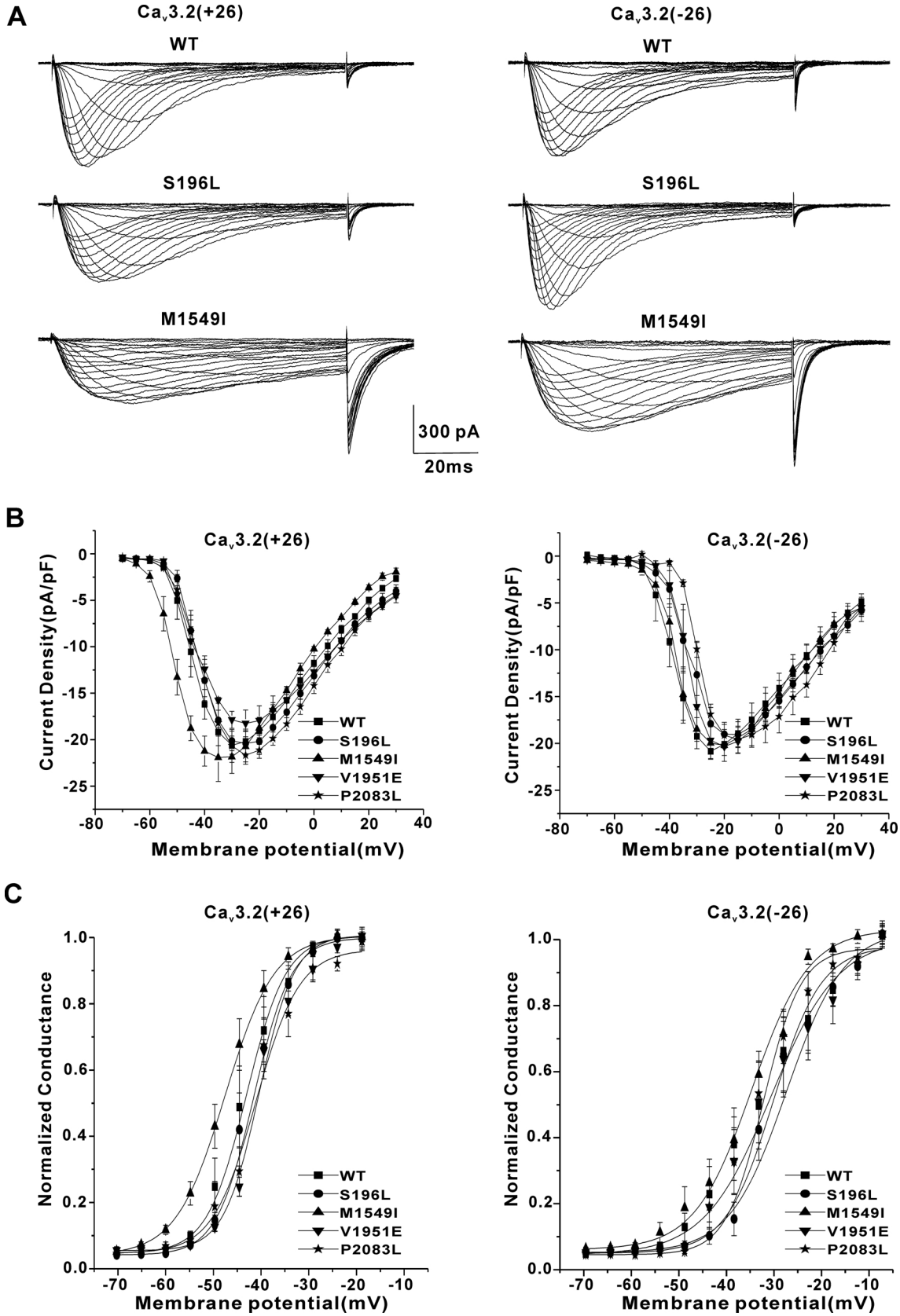

Fig. 2. Effects of the **S196 L, M1549I, V1951E and P2083L** mutations on the current densities and the activation properties of $Ca_V3.2(\pm 26)$ splice variants in HEK293 cells. (A) Representative Ca^{2+} current traces showing the effects of the S196 L and M1549I mutations on $Ca_V3.2(\pm 26)$ channels expressed in HEK293 cells. (B) Current–voltage relationship (I–V curves) generated from peak current density at each test voltage. (Data are presented as means ± SEM, n = 7–11). (C) The effects of the four primary aldosteronism mutations on the steady-state activation of Cav3.2 (± 26) currents. The normalized data points were fitted using a Boltzmann equation. (n = 7–11).

Table 1
Effects of the four PA mutations on the current densities and the activation properties of $Ca_V3.2(\pm 26)$ currents.

$Ca_V3.2(+26)$	WT	S196L	M1549I	V1951E	P2083L
Activation $V_{1/2}$(mV)	−43.5 ± 0.7(11)	−42.8 ± 0.3(7)	−48.7 ± 1.3(9)*	−41.0 ± 2.4(8)	−41.6 ± 2.8(10)
Activation slope(mV)	3.5 ± 0.7(11)	3.3 ± 0.5(7)	3.2 ± 0.8(10)	3.9 ± 0.6(8)	3.9 ± 1.0(10)
Tau act(ms) @−30 mV	5.6 ± 1.0(10)	6.1 ± 0.9(6)	12.8 ± 4.3(6)**	7.1 ± 1.1(6)	8.7 ± 1.4(7)*
Current density(pA/pF)	−20.6 ± 0.9(8)	−20.4 ± 1.3(11)	−21.9 ± 2.6(9)	−18.7 ± 1.4(6)	−21.7 ± 1.0(11)
$Ca_V3.2(-26)$	WT	S196L	M1549I	V1951E	P2083L
Activation $V_{1/2}$(mV)	−35.3 ± 2.4(11)	−31.5 ± 4.5(11)	−37.6 ± 1.2(16)	−35.2 ± 1.0(11)	−36.4 ± 3.9(18)
Activation slope(mV)	4.9 ± 0.7(11)	5.1 ± 0.4(11)	4.6 ± 0.7(16)	5.3 ± 0.6(11)	5.1 ± 0.9(18)
Tau act(ms)@−30 mV	5.3 ± 1.8(11)	8.0 ± 2.7(11)	13.1 ± 2.0(9)**	5.1 ± 0.9(9)	3.8 ± 0.5(14)
Current density(pA/pF)	−20.8 ± 0.8(9)	−19.1 ± 0.8(8)	−20.2 ± 1.7(10)	−20.3 ± 1.3(9)	−19.6 ± 1.4(15)

Numbers in brackets are cells recorded for each condition.
*, $P < 0.05$; **, $P < 0.01$, compared with wild-type channels.

Table 2) from above I–V recordings revealed markedly alteration in inactivation kinetics of $Ca_V3.2(+26)^{M1549I}$ and $Ca_V3.2(-26)^{M1549I}$ currents. The M1549 mutation increased the inactivation time constant of $Ca_V3.2(+26)$ and $Ca_V3.2(-26)$ by more than 5 and 2 folds respectively (Table 2). The S196 L mutation also increased the inactivation time constant of $Ca_V3.2(+26)$ currents, but did not alter the inactivation time constant of $Ca_V3.2(-26)$ currents (Table 2). Both the V1951E and P2083 L mutations did not change the inactivation time constant of either $Ca_V3.2(+26)$ or $Ca_V3.2(-26)$ currents (Table 2).

The steady-state channel inactivation was studied using tail currents in response to test potential at −20 mV (6 ms) from a pre-pulse incremented in 5 mV (−90 mV to -25 mV; 6 s) upon repolarization to −70 mV (Fig. 3). The half-maximal voltage dependence of inactivation for $Ca_V3.2(+26)$ or $Ca_V3.2(-26)$ currents was unaffected by the S196 L, V1951E and P2083 L mutations (Fig. 3, Table2). The M1549I mutation altered the steady-state inactivation of $Ca_V3.2(+26)$ currents, but had no effect on $Ca_V3.2(-26)$ currents(Table 2). The time course for deactivation(Tau deact) was analyzed by fitting the tail currents with a single exponential standard equation. The S196 L, V1951E and P2083 L mutations did not alter the deactivation kinetics of $Ca_V3.2(\pm 26)$ channel currents, while the M1549I mutation increased the deactivation time constant of $Ca_V3.2(+26)$ and $Ca_V3.2(-26)$ by around 6 and 4 folds respectively (Table 2). These data suggested that the M1549I mutations have more profound effects on the inactivation and deactivation properties of $Ca_V3.2(\pm 26)$ currents than the other three mutations.

3.3. Effects of the four mutations on the recovery from inactivation of $Ca_V3.2$ channel currents

Finally, we investigated the effects of the four PA mutations on the recovery from inactivation of $Ca_V3.2$ channel currents. Recovery from inactivation was studied by using a double pulse protocol (holding at −90 mV, first a 400 ms pulse to −30 mV, then a 50 ms pulse to −30 mV, the time between pulses varying from 50 ms to 7 s). Fig. 4A showed typical recordings from HEK293 cells transfected with wide-type $Ca_V3.2(\pm 26)$, S196 L and M1549I mutant $Ca_V3.2(\pm 26)$ channels. As shown in Fig. 4B and C, the V1951E, S196 L and P2083 L mutations significantly promoted $Ca_V3.2(+26)$ channel recovery from inactivation, while M1549I mutation slowed the channel recovery from inactivation (Tau recovery: WT $Ca_V3.2(+26)$: 657.8 ± 93.0 ms; $Ca_V3.2(+26)^{S196L}$: 479.3 ± 85.4 ms; $Ca_V3.2(+26)^{V1951E}$: 225.2 ± 85.1 ms; $Ca_V3.2(+26)^{P2083L}$: 250.5 ± 55.3 ms; $Ca_V3.2(+26)^{M1549I}$: 1161.1 ± 131.1 ms; $P < 0.05$ compared to WT, n = 6–11). These data indicated that V1951E, S196 L and P2083 L mutations may increase $Ca_V3.2(+26)$ availability during repetitive electrical activities. Interestingly, all four mutations did not have significantly effects on the recovery from inactivation of $Ca_V3.2(-26)$ channels (Fig. 4B and C). Therefore, the data of recovery from inactivation properties, again, suggested that the four PA mutations have more profound effects on $Ca_V3.2(+26)$ currents than on $Ca_V3.2(-26)$.

3.4. Effects of the four mutations on high K^+-stimulated aldosterone secretion in H295R cells

Angiotensin II (Ang II) and potassium are the two primary physiologic aldosterone secretagogues. Voltage-gated $Ca_V3.2$ channels were shown to be mainly involved in high K^+ -stimulated aldosterone secretion in H295R cells [5]. Therefore, we tested high K^+(15 mM)-stimulated aldosterone secretion in H295R cells transfected with wild-type and mutant $Ca_V3.2(+26)$ channels. As shown in Fig. 5A, all four mutant channels increased high K^+-stimulated aldosterone secretion in H295R cells. Steroidogenic acute regulatory protein (STAR) and aldosterone synthase (CYP11B2) are key steroidogenic proteins, which control the early and late rate-limiting steps in aldosterone biosynthesis respectively. The S196 L and M1549I mutations increased the mRNA

Table 2
Effects of the four PA mutations on the inactivation and deactivation properties of $Ca_V3.2(\pm 26)$ currents.

$Ca_V3.2(+26)$	WT	S196L	M1549I	V1951E	P2083L
Inactivation $V_{1/2}$(mV)	−59.5 ± 0.4(19)	−60.6 ± 0.5(16)	−64.3 ± 0.7(13)*	−56.7 ± 1.2(12)	−57.0 ± 1.0(15)
Inactivation slope(mV)	4.0 ± 0.9(15)	4.2 ± 1.0(13)	4.1 ± 0.5(10)	4.0 ± 0.9(9)	4.0 ± 0.4(12)
Tau inact(ms)@−30 mV	20.5 ± 1.1(13)	36.9 ± 1.3(13)**	112.5 ± 11.3(8)**	18.3 ± 3.7(7)	19.9 ± 1.2(8)
Tau deact(ms)@-70mV	2.8 ± 0.4(11)	3.2 ± 0.9(10)	16.4 ± 2.3(10)***	3.2 ± 0.2(8)	2.7 ± 0.1(12)
$Ca_V3.2(-26)$	WT	S196L	M1549I	V1951E	P2083L
Inactivation $V_{1/2}$(mV)	−51.0 ± 0.7(25)	−52.9 ± 0.9(17)	−53.1 ± 0.6(9)	−52.2 ± 1.1(13)	−50.5 ± 0.7(21)
Inactivation slope(mV)	4.1 ± 1.1(21)	4.0 ± 0.6(14)	3.9 ± 0.5(7)	4.2 ± 0.6(10)	3.5 ± 0.7(17)
Tau inact(ms)@−30 mV	19.4 ± 1.3(11)	15.5 ± 1.7(12)	49.0 ± 4.3(7)**	17.0 ± 2.2(10)	16.4 ± 1.1(16)
Tau deact(ms)@-70mV	2.2 ± 0.2(15)	2.1 ± 0.1(11)	9.2 ± 1.1(7)**	2.3 ± 0.2(8)	2.2 ± 0.2(13)

Numbers in brackets are cells recorded for each condition.
*, $P < 0.05$; **, $P < 0.01$; ***, $P < 0.001$, compared with wild-type channels.

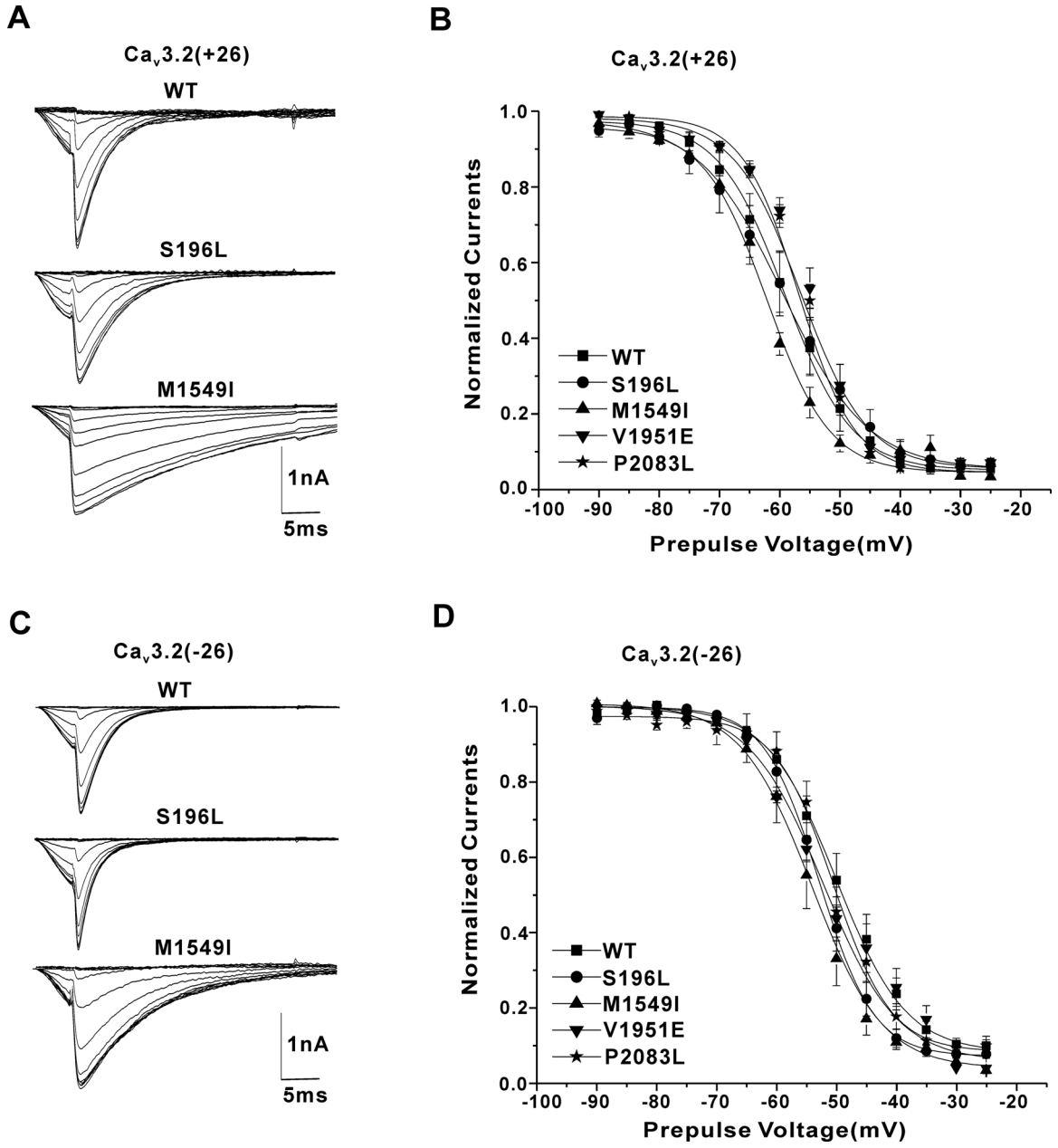

Fig. 3. Effects of the **S196 L, M1549I, V1951E and P2083**L mutations on the steady-state inactivation of CaV3.2(± 26) splice variants in HEK293 cells. (A) Representative current traces showing the effects of the S196 L and M1549I mutations on the voltage-dependence of inactivation of Cav3.2(+ 26) currents. (B) The effects of the four mutations on the steady-state inactivation of Cav3.2(+ 26) currents. Normalized data points were fitted using a Boltzmann equation. (C) The current traces show the effects of the S196 L and M1549I mutations on the voltage-dependence of inactivation of Cav3.2(-26). (D) The effects of the four mutations on the steady-state inactivation of Cav3.2(-26) currents. (n = 7–25).

expression of both STAR and CYP11B2 (Fig. 5). The V1951E and P2083 L mutations significantly increased the mRNA expression of CYP11B2 and STAR respectively (Fig. 5). These data suggested that the four PA mutations are associated with the overproduction of aldosterone in PA patients.

4. Discussion

In this study we found that human ZG cells express $Ca_V3.2(+26)$ but not $Ca_V3.2(-26)$ splice variant. Interestingly, the S196 L, M1549I, V1951E and P2083 L mutations had more profound effects on $Ca_V3.2(+26)$ than $Ca_V3.2(-26)$ channels expressed in HEK293 cells. The M1549I mutation is located in a conserved site in the S6 helix that regulates T-type calcium channel inactivation [17,18]. In consistence with the previous report [5], we found that $Ca_V3.2(+26)^{M1549I}$ mutant channels inactivated dramatically slower and activated at more hyperpolarized potentials, which make channels more likely to open at membrane potentials close to the resting membrane potential and keep open longer, leading to more calcium entry into ZG cells, resulting in overproduction of aldosterone [19]. Our previous study suggested that human ZG cells may spontaneously generate membrane potential oscillations [20]. The S196 L, V1951E and P2083 L mutations dramatically promoted $Ca_V3.2(+26)$ channel recovery from inactivation, which could lead to increased calcium influx and aldosterone secretion during the repetitive channel activities [5,20]. Human brain expresses both $Ca_V3.2(+26)$ and $Ca_V3.2(-26)$ splice isoforms [21]. We found that except the M1549I mutation, the V1951E, S196 L and P2083 L have little effect on electrophysiological properties of $Ca_V3.2(-26)$ channels,

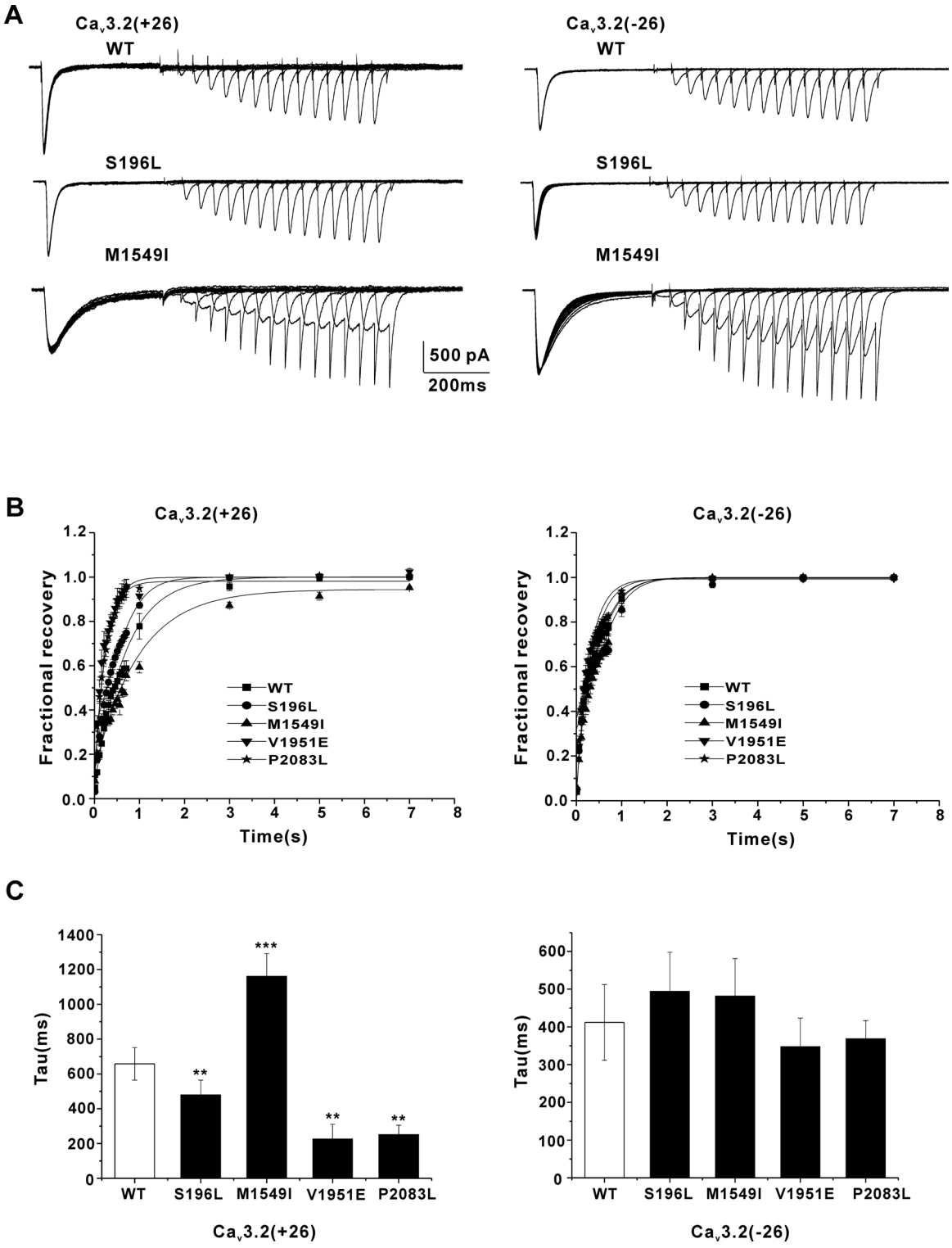

Fig. 4. Effects of the **S196 L, M1549I, V1951E and P2083L** mutations on the recovery from inactivation of CaV3.2(± 26) splice variants in HEK293 cells. (A) Representative Ca^{2+} current traces obtained by a double pulse protocol (holding at −90 mV, first a 400 ms pulse to −30 mV, then a 50 ms pulse to −30 mV, the time between pulses varying from 50 ms to 7 s). (B) The effects of the four mutations on fractional recovery of CaV3.2(± 26). (C) All four mutations significantly changed the recovery from inactivation of CaV3.2(+26) currents, but not CaV3.2(-26) currents. (n = 6–11). **, P < 0.01; ***, P < 0.001, compared with wild-type channels.

which may partially explain why the four PA mutations have different clinical manifestations (ie, only patients with M1549I mutation show neuronal abnormalities besides PA).

Moreover, our data suggested that long isoforms of $Ca_V3.2$ splice variants may be more sensitive to point mutations than short ones. In consistence with our findings, Powell et al reported that the R1584 P mutation caused greater electrophysiological changes in rat $Ca_V3.2(+25)$ than $Ca_V3.2(-25)$ expressed in HEK293 cells [11]. Besides $Ca_V3.2$ channels, splice-variant specific effects of point mutations were also found in $Ca_V2.1$ channels. Adsmas et al reported that the human

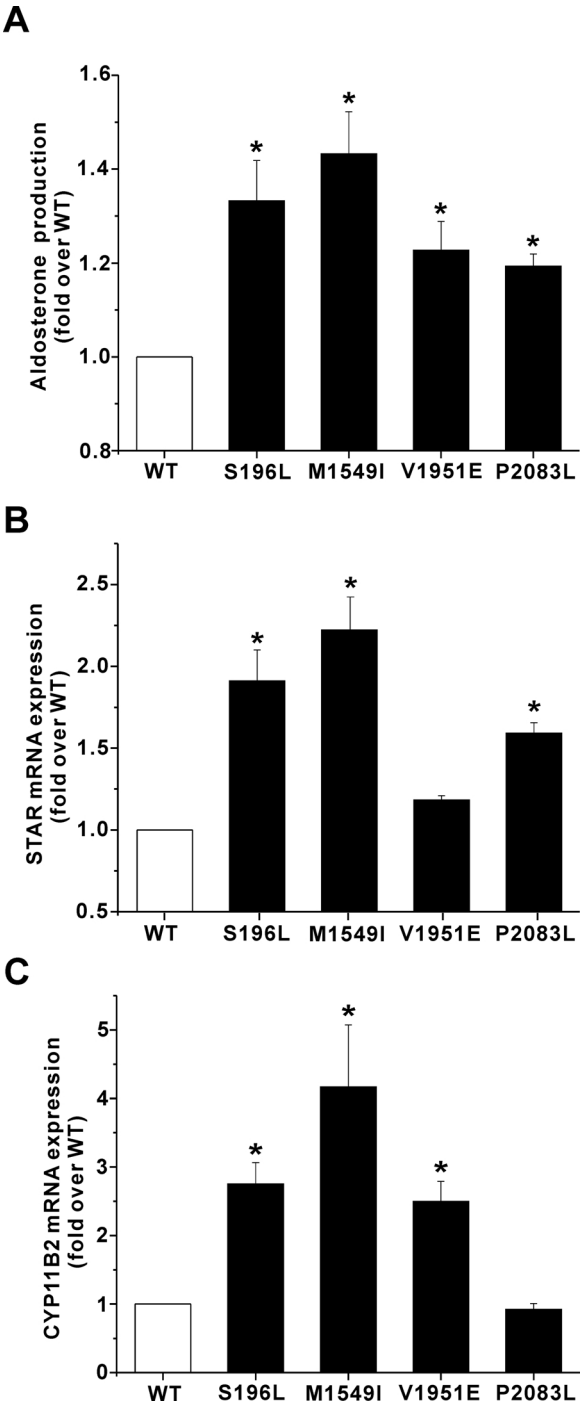

Fig. 5. Effects of the **S196 L, M1549I, V1951E and P2083L** mutations on high K^+-stimulated aldosterone secretion in H295R cells. (A) The four mutations increased high K^+-stimulated aldosterone secretion in H295R cells. (B and C) The effects of the four mutations on mRNA expression of the key proteins that control steroid biosynthesis: STAR and CYP11B2. Data are presented as fold-change over wild-type. *, $P < 0.05$ compared with cells transfected with wild-type $Ca_V3.2(+26)$ channels. (n = 3).

familial hemiplegic migraine mutations K1336E, R192Q and S218 L caused a greater left shift of the activation curves of the short $Ca_V2.1$ isoform (with exon 47) than the long isoform (without exon 47) expressed in HEK293 cells [22]. A recent study showed that the K165R mutation significantly changed the reverse potential of rabbit $Ca_V1.1e$ (without exon 29) around 10 mV, while did no alter the reverse potential of $Ca_V1.1a$ isoform(without exon 29) [23]. These data suggest that splice-variant specific effects of point mutations may be a common phenomenon among voltage-gated calcium channels.

In conclusion, our results provide the first evidence that: (a) Human ZG cells express $Ca_V3.2(+26)$ but not $Ca_V3.2(-26)$ splice variant. (b) The four PA mutations have splice-variant specific effects on human $Ca_V3.2$ channels. Our results indicate that *CACNA1H* gene mutations produce obvious functional effects only on specific splice variants, and that genetic mutations of voltage-gated calcium channels may produce cell-type specific effects depending on splice variant expression patterns.

Author contributions

Conception and design of the experiments: C.H; collection of the data: M.H, Y.Z and X.Z; analysis and interpretation of the data: M.H, Y.Z, X.Z and C.H.; drafting the article or revising it critically for important intellectual content: C.H, M.H and Z.X

Declaration of Competing Interest

None.

Acknowledgements

This work was supported by the National Key R&D Program of China (2016YFA0100802), the National Natural Science Foundation of China (NSFC 31771282 and31271240)

References

[1] E. Perez-Reyes, Molecular physiology of low-voltage-activated t-type calcium channels, Physiol. Rev. 83 (2003) 117–161.
[2] G. Santoni, M. Santoni, M. Nabissi, Functional role of T-type calcium channels in tumour growth and progression: prospective in cancer therapy, Br. J. Pharmacol. 166 (2012) 1244–1246.
[3] S.M. Cain, T.P. Snutch, T-type calcium channels in burst-firing, network synchrony, and epilepsy, Biochim. Biophys. Acta 1828 (2013) 1572–1578.
[4] T. Yang, M. He, C. Hu, Regulation of aldosterone production by ion channels: from basal secretion to primary aldosteronism, Biochim. Biophys. Acta 1864 (2018) 871–881.
[5] G. Daniil, F.L. Fernandes-Rosa, J. Chemin, I. Blesneac, J. Beltrand, M. Polak, X. Jeunemaitre, S. Boulkroun, L. Amar, T.M. Strom, P. Lory, M.C. Zennaro, CACNA1H mutations are associated with different forms of primary aldosteronism, EBioMedicine 13 (2016) 225–236.
[6] P.J. Adams, T.P. Snutch, Calcium channelopathies: voltage-gated calcium channels, Subcell. Biochem. 45 (2007) 215–251.
[7] D. Lipscombe, A. Andrade, S.E. Allen, Alternative splicing: functional diversity among voltage-gated calcium channels and behavioral consequences, Biochim. Biophys. Acta 1828 (2013) 1522–1529.
[8] H. Seitter, A. Koschak, Relevance of tissue specific subunit expression in channelopathies, Neuropharmacology 132 (2018) 58–70.
[9] C.J. Jeng, Y.T. Chen, Y.W. Chen, C.Y. Tang, Dominant-negative effects of human P/Q-type Ca2+ channel mutations associated with episodic ataxia type 2, Am. J. Physiol. Cell Physiol. 290 (2006) C1209–1220.
[10] L.S. David, E. Garcia, S.M. Cain, E. Thau, J.R. Tyson, T.P. Snutch, Splice-variant changes of the Ca(V)3.2 T-type calcium channel mediate voltage-dependent facilitation and associate with cardiac hypertrophy and development, Channels (Austin) 4 (2010) 375–389.
[11] K.L. Powell, S.M. Cain, C. Ng, S. Sirdesai, L.S. David, M. Kyi, E. Garcia, J.R. Tyson, C.A. Reid, M. Bahlo, S.J. Foote, T.P. Snutch, T.J. O'Brien, A Cav3.2 T-type calcium channel point mutation has splice-variant-specific effects on function and segregates with seizure expression in a polygenic rat model of absence epilepsy, J. Neurosci. 29 (2009) 371–380.
[12] T. Ohkubo, Y. Inoue, T. Kawarabayashi, K. Kitamura, Identification and electrophysiological characteristics of isoforms of T-type calcium channel Ca(v)3.2 expressed in pregnant human uterus, Cell. Physiol. Biochem. 16 (2005) 245–254.
[13] S. Jagannathan, E.L. Punt, Y. Gu, C. Arnoult, D. Sakkas, C.L. Barratt, S.J. Publicover, Identification and localization of T-type voltage-operated calcium channel subunits in human male germ cells. Expression of multiple isoforms, J. Biol. Chem. 277 (2002) 8449–8456.
[14] T. Yang, H.L. Zhang, Q. Liang, Y. Shi, Y.A. Mei, P.Q. Barrett, C. Hu, Small-conductance Ca2+-Activated potassium channels negatively regulate aldosterone secretion in human adrenocortical cells, Hypertension 68 (2016) 785–795.
[15] Y. Cui, X. Liu, T. Yang, Y.A. Mei, C. Hu, Exposure to extremely low-frequency electromagnetic fields inhibits T-type calcium channels via AA/LTE4 signaling pathway, Cell Calcium 55 (2014) 48–58.

[16] W.E. Rainey, K. Saner, B.P. Schimmer, Adrenocortical cell lines, Mol. Cell. Endocrinol. 228 (2004) 23–38.
[17] R. Marksteiner, P. Schurr, S. Berjukow, E. Margreiter, E. Perez-Reyes, S. Hering, Inactivation determinants in segment IIIS6 of Ca(v)3.1, J. Physiol. 537 (2001) 27–34.
[18] U.I. Scholl, G. Stolting, C. Nelson-Williams, A.A. Vichot, M. Choi, E. Loring, M.L. Prasad, G. Goh, T. Carling, C.C. Juhlin, I. Quack, L.C. Rump, A. Thiel, M. Lande, B.G. Frazier, M. Rasoulpour, D.L. Bowlin, C.B. Sethna, H. Trachtman, C. Fahlke, R.P. Lifton, Recurrent gain of function mutation in calcium channel CACNA1H causes early-onset hypertension with primary aldosteronism, Elife 4 (2015) e06315.
[19] P.Q. Barrett, N.A. Guagliardo, P.M. Klein, C. Hu, D.T. Breault, M.P. Beenhakker, Role of voltage-gated calcium channels in the regulation of aldosterone production from zona glomerulosa cells of the adrenal cortex, J. Physiol. 594 (2016) 5851–5860.
[20] C. Hu, C.G. Rusin, Z. Tan, N.A. Guagliardo, P.Q. Barrett, Zona glomerulosa cells of the mouse adrenal cortex are intrinsic electrical oscillators, J. Clin. Invest. 122 (2012) 2046–2053.
[21] X. Zhong, J.R. Liu, J.W. Kyle, D.A. Hanck, W.S. Agnew, A profile of alternative RNA splicing and transcript variation of CACNA1H, a human T-channel gene candidate for idiopathic generalized epilepsies, Hum. Mol. Genet. 15 (2006) 1497–1512.
[22] P.J. Adams, E. Garcia, L.S. David, K.J. Mulatz, S.D. Spacey, T.P. Snutch, Ca(V)2.1 P/Q-type calcium channel alternative splicing affects the functional impact of familial hemiplegic migraine mutations: implications for calcium channelopathies, Channels (Austin) 3 (2009) 110–121.
[23] Y. El Ghaleb, M. Campiglio, B.E. Flucher, Correcting the R165K substitution in the first voltage-sensor of CaV1.1 right-shifts the voltage-dependence of skeletal muscle calcium channel activation, Channels (Austin) 13 (2019) 62–71.